Proceedings of the 2011 IEEE
International Conference on Robotics and Biomimetics
December 7-11, 2011, Phuket, Thailand

A Pilot Investigation of Continuum Robots as a Design Alternative for Upper Extremity Exoskeletons

Kai Xu*, *Member, IEEE*, Dong Qiu, *Student Member, IEEE*, Nabil Simaan, *Member, IEEE*

***Abstract*—Most existing exoskeletons have followed a similar design approach using articulated rigid links, despite the applications of strength augmentation or rehabilitation, which may have very different specifications. In order to address the urge for ergonomics in wearable assistive exoskeletons for rehabilitation, this paper proposed a design alternative using compliant continuum mechanisms. Design concepts were elaborated for an upper extremity exoskeleton for a shoulder joint. Design considerations were then detailed based on a general kinematics and statics model extended from previously published results. Construction, actuation and transmission schemes for a selected continuum structure were discussed and a preliminary prototype was constructed to demonstrate feasibility of the proposed idea.**

I. Introduction

EXOSKELETON research attracted significant attentions in the past decades. Numerous exoskeleton systems have been developed for upper and lower limbs, for military and medical applications (e.g. [1, 2]). These exoskeleton systems either seek to augment a healthy wearer's physical capability with robotic actuation for enhanced strength and stamina or to allow rehabilitation of neuromuscular defects after stroke or neural injury. Examples include the Mihailo Pupin Institute exoskeleton for rehabilitation of paraplegics [3] from the 70s and many recent advances, such as performance-augmenting full-body exoskeleton systems [4-6] from UC Berkeley, load-carrying lower extremity exoskeletons from MIT [7, 8], rehabilitation exoskeletons for lower limbs [9-12], and upper limbs [13-21]. Most of the aforementioned systems use actuation of hydraulic [7] or pneumatic cylinders [3, 9, 20], rotary pneumatic actuators [5], pneumatic muscle actuators [13], cable actuations [11, 14], parallel mechanisms [12, 16, 19], gearmotors [4, 15], linkages [18, 21], etc.

Besides these actual exoskeleton systems, research is also about enabling technologies, such as inertia compensation [22], sensing & control [4, 8, 23, 24], discomfort reduction [25], hyperstaticity avoidance [26], new actuators [27], rehabilitation treatment planning [28, 29], etc.

Among existing wearable exoskeletons designs, most have followed one similar design approach: articulated rigid links are actuated with a human wearer attached. Regardless the applications (rehabilitation or strength augmentation), these designs have essentially similar topological structures, with different sensing and actuation methods.

The use of rigid links in an exoskeleton design, which may be suitable for applications requiring strength augmentation, has many disadvantages for applications emphasizing user comfort with a low to moderate force requirement. One such application is rehabilitation where ergonomics, low inertia, device compactness, and conformity to human shapes are paramount. A design with compliant components might lead to better outcomes. Such design attempts include a simulation by van den Bogert to show the possibility of using elastic cords to assist walking [30], an upper body exoskeleton using home-made pneumatic artificial muscles by Kobayashi *et al.* [31], and a cable-driven upper extremity exoskeleton by Agrawal *et al.* [32, 33]. The use of continuum mechanisms to address this design challenge has not been explored yet.

This paper presents an alternative design of rehabilitation exoskeletons using continuum mechanisms as shown in Fig. 1. Bending of the continuum mechanism (Fig. 1.(2)) orients the upper arm accordingly.

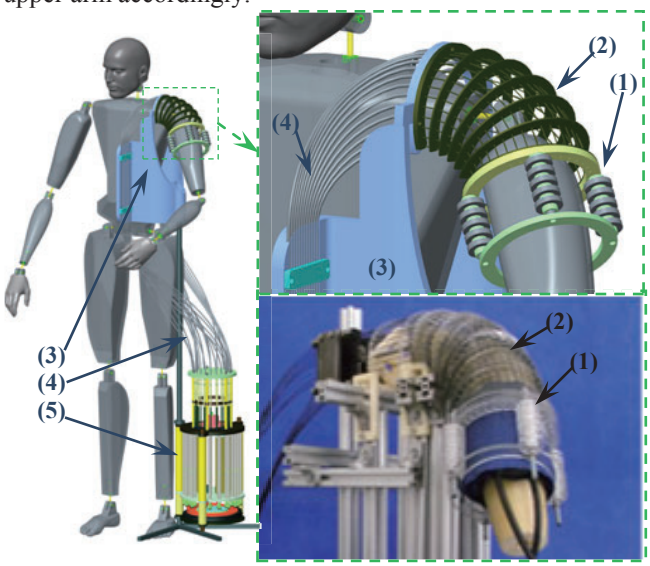

Fig. 1. Upper extremity exoskeleton using continuum mechanisms: (1) a rigid upper arm sleeve, (2) a flexible continuum joint brace, (3) a body vest, (4) a set of guiding cannulae, and (5) an actuation unit

The paper's main contribution is in investigating this novel

Manuscript received Mar 14th, 2011. This work was supported by the Chinese Ministry of Education Program for New Century Excellent Talents in University (NCET Program).

Kai Xu is with R.I.I Lab, UM-SJTU Joint Institute, Shanghai Jiao Tong University, Shanghai, 200240, China (corresponding author, phone: 86-21-3420-7220; fax: 86-21-3420-6525; email: k.xu@sjtu.edu.cn)

Qong Qiu is with R.I.I Lab, UM-SJTU Joint Institute, Shanghai Jiao Tong University, Shanghai, 200240, China (email: dongqiu@sjtu.edu.cn)

Nabil Simaan is with A.R.M.A Lab, Department of Mechanical Engineering, Vanderbilt University, Nashville, Tennessee, 37235, USA (email: nabil.simaan@vanderbilt.edu)

978-1-4577-2138-0/11/$26.00 © 2011 IEEE

concept while focusing on design considerations such as kinematics and statics modeling, constructions and actuation schemes. The concept is verified using a preliminary prototype. Other contributions of this paper include 1) derivation of kinematics and statics modeling for the continuum structure with arbitrary placement of secondary backbones and 2) a design of a hydraulic transmission which can drive multiple secondary backbones simultaneously.

The paper is organized as the following. Section II covers the design concept and a design overview. Section III presents nomenclature, kinematics and statics modeling to facilitate the explanation of design components in Section VI. Section V presents a preliminary prototype for demonstration with conclusions followed in Section VI.

II. Design Concept and Overview

The design concept shown in Fig. 1 uses a flexible joint brace (Fig. 1.#2) to orient a patient's humerus. This work is inspired by [34-36] where continuum architectures as in Fig. 2.(a) were designed and used as dexterous wrists for a surgical slave. This continuum structure in Fig. 2-(a) consists of an end disk, a base disk, a few secondary backbones and a primary backbone. All the backbones are made from thin NiTi (Nickel-Titanium alloy) rods. The primary backbone is attached to both the end disk and the base disk, while secondary backbones are only attached to the end disk and can slide in holes of the base disk. A 2-DoF (Degree of Freedom) bending of the continuum structure is achieved by simultaneously pulling and pushing all the secondary backbones. Major advantages of this structure include: 1) scalability, 2) actuation redundancy introduced by using multiple secondary backbones to drive a 2-DoF bending that loads on backbones can be redistributed and buckling risks can be minimized, and 3) design compactness achieved by dual roles of these secondary backbones as both structural components and actuation members. More importantly, inherent compliance of this continuum structure is particularly advantageous for rehabilitation purposes which could greatly increase user comfort and safety.

Our current design and a preliminary prototype for a mockup shoulder joint is shown in Fig. 1. It consists of a rigid upper arm sleeve (#1), a flexible continuum joint brace (#2), a body vest (#3), a set of rigid guiding cannulae (#4), and an actuation unit (#5).

The continuum joint brace (Fig. 1.#2) has multiple secondary backbones made from thin NiTi rods. The primary backbone is eliminated to provide space for the upper arm. Multiple spacer disks are integrated in the structure to reduce backbones' buckling risks. A flexible mesh is used to keep these spacer disks evenly distributed. The actuation unit (Fig. 1.#5) pulls and pushes these secondary backbones that are routed through a set of rigid guiding cannulae (Fig. 1.#4) embedded in the body vest (Fig. 1.#3). The continuum brace could have many different forms with various number and placement of the secondary backbones. Choices are made based on statics and stress analysis presented in Section IV.

The flexible continuum joint brace (Fig. 1.#2) only has 2 DoFs while a human shoulder joint can be approximated by a 3-DoF spherical joint. A rotation along the axis of the upper arm is not assisted by the current design. Small wheels are assembled to the rigid upper arm sleeve (Fig. 1.#1) so that the upper arm can rotate freely with respect to the upper arm sleeve. Actual implementation includes an inflatable bandage to fill up the space between the sleeve and the upper arm, as shown in Fig. 1 and Fig. 7.

Bending of the continuum joint brace will orient the upper arm sleeve as desired. The bending is achieved by pushing and pulling all the NiTi secondary backbones simultaneously. Exact orientation and shape of the arm sleeve depends on a minimal potential energy solution of the elastic potential energy of the NiTi rods and the gravitational potential energy of the arm sleeve and the patient's limb, constrained by the patient's anatomical geometry. Exact modeling of this system will be difficult but fortunately absolute motion accuracy is less of concern in many rehabilitation applications.

Although the current design is only for the shoulder joint, more continuum mechanisms could be stacked to build a multiple-DoF exoskeleton to assist an entire upper arm. The ultimate goal is to build an exoskeleton for rehabilitation with a light and compliant wearable part and superb comfort.

III. Theoretical Background

Modeling of the continuum structure as in Fig. 2 has been studied in many works (e.g. [35-39]). An approximation widely accepted and experimentally validated assumes each NiTi backbone bending into a circular shape [40]. Following this assumption, coordinates and nomenclatures are defined to facilitate the kinematic modeling.

This paper extends the kinematics and statics modeling from [34, 35, 39] to include cases where the continuum structure may have an arbitrary number and placement of the secondary backbones.

A. Coordinates and nomenclature

As shown in Fig. 2, four coordinates are defined and nomenclature is defined in Table I.

- *Base Disk Coordinate System* (BDS) $\{b\} \equiv \{\hat{\mathbf{x}}_b, \mathbf{y}_b, \mathbf{z}_b\}$ is attached to the base disk with its XY plane coinciding with the base disk and its origin at the center. The $\hat{\mathbf{x}}_b$ points from the center of the base disk to the first secondary backbone while the $\hat{\mathbf{z}}_b$ is perpendicular to the base disk. Secondary backbones are numbered according to the definition of δ_i.
- *Bending Plane Coordinate System 1* (BPS1) $\{c\} \equiv \{\hat{\mathbf{x}}_c, \mathbf{y}_c, \mathbf{z}_c\}$ is defined such that the continuum segment bends in the XZ plane, with its origin coinciding with the origin of $\{b\}$.
- *Bending Plane Coordinate System 2* (BPS2) $\{d\} \equiv \{\hat{\mathbf{x}}_d, \mathbf{y}_d, \mathbf{z}_d\}$ is obtained from $\{c\}$ by a rotation

about $\hat{\mathbf{y}}_c$ such that $\hat{\mathbf{z}}_c$ becomes the backbone tangent at the center of the end disk.

- *End Disk Coordinate System* (EDS) $\{e\} \equiv \{\hat{\mathbf{x}}_e, \mathbf{y}_e, \mathbf{z}_e\}$ is attached to the end disk. $\hat{\mathbf{x}}_e$ points from the center to the *1*st secondary backbone with $\hat{\mathbf{z}}_e$ normal to the end disk. $\{e\}$ is obtained by a rotation about $\hat{\mathbf{z}}_d$ from $\{d\}$.

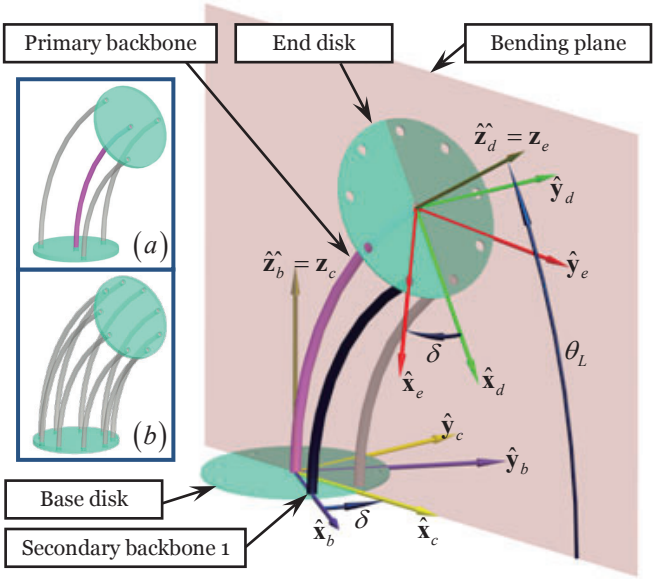

Fig. 2. Kinematics nomenclature: (a) the structure used in [34-36], (b) a structure with multiple secondary backbones

TABLE I: NOMENCLATURE USED

m	Number of the secondary backbones.
i	Index of the secondary backbones, $i=1,2,\cdots,m$
r_i	Distance from the primary to the ith secondary backbone. r_i doesn't have to be the same for all the secondary backbones.
E_p, E_i	Young's modulus of the primary and the secondary backbones
I_p, I_i	Cross-sectional moment of inertia of the primary and the secondary backbones
L_p	Length of the primary backbone. In the absence of a primary backbone, it is the length when the structure is straight (at this moment, all the secondary backbones have the same length).
L_i	Length of the ith secondary backbone.
$\mathbf{q}$	$\mathbf{q}=[q_1\ q_2\ \cdots\ q_m]^T$ is]the actuation length vector of the secondary backbones, where $q_i=L_i-L_p$
$\theta(s)$	The angle of the tangent to the primary backbone in the bending plane along the arc. $\theta(L_p)$ and $\theta(0)$ are designated by θ_L and θ_0. $\theta_0=\pi/2$ is a constant.
δ_i	A right-handed rotation angle from $\hat{\mathbf{x}}_c$ about $\hat{\mathbf{z}}_c$ to a line passing through the primary backbone and the ith secondary backbone. δ_i doesn't have to be evenly distributed.
δ	$\delta \equiv \delta_1$ and $\delta_i=\delta+\beta_i$. Once the continuum structure is built, all the β_i are constants.
$\boldsymbol{\psi}$	$\boldsymbol{\psi}=[\theta_L\ \delta]^T$ defines a configuration of the continuum brace.
$\boldsymbol{\tau}$	$\boldsymbol{\tau}=[\tau_1\ \tau_2\ \cdots\tau_m]^T$ is the actuation force vector of the secondary backbones.
$\mathbf{J}_{x\psi}$	$\dot{\mathbf{x}}=\dot{\boldsymbol{\psi}}\mathbf{J}_{x\psi}^T$ where $\dot{\mathbf{x}}$ is the twist of the end disk in $\{b\}$. In $\dot{\mathbf{x}}$, the linear velocity precedes the angular velocity.
$\mathbf{J}_{q\psi}$	Jacobian matrix of the mapping $\dot{\mathbf{q}}=\dot{\boldsymbol{\psi}}\mathbf{J}_{q\psi}^T$
E	Elastic energy of the continuum structure.
$\mathbf{W}_e$	$\mathbf{W}_e=[\mathbf{f}_e^T\ \mathbf{m}_e^T]^T$ is an external wrench with force components preceding moment components.

B. Kinematics and statics

The orientation of the continuum brace is characterized by $\boldsymbol{\psi}=[\theta_L\ \delta]^T$. Proper actuation of q_i will orient the upper arm as desired while τ_i will guide the design of the actuation unit. Based on derivations detailed in [35, 36, 39], expressions of q_i and τ_i have been generalized to include cases where r_i and δ_i can have arbitrary values:

$$q_i = r_i \cos\delta_i \left(\theta_L - \theta_0\right) \tag{1}$$

$$\boldsymbol{\tau}\mathbf{J}_{q\psi x\psi}^{T} = \left(\quad\right)^{+} \left(\nabla E - \mathbf{W}_e^{T} \quad\right) \tag{2}$$

Where entities are derived as the following:

$$\mathbf{J}_{q\psi} = \begin{bmatrix} r_1\cos\delta_1 & -r_1\left(\theta_L-\theta_0\right)\sin\delta_1 \\ r_2\cos\delta_2 & -r_2\left(\theta_L-\theta_0\right)\sin\delta_2 \\ \vdots & \vdots \\ r_m\cos\delta_m & -r_m\left(\theta_L-\theta_0\right)\sin\delta_m \end{bmatrix} \tag{3}$$

$$E = \frac{\left(\theta_L-\theta_0\right)^2}{2}\left(\frac{EI_p}{L_p}+\sum_{i=1}^{m}\frac{EI_i}{L_i}\right) \tag{4}$$

$$\nabla E = \begin{bmatrix} \left(\theta_L-\theta_0\right)\left(\dfrac{EI_p}{L_p}+\displaystyle\sum_{i=1}^{m}\frac{EI_i}{L_i}\right) - \dfrac{\left(\theta_L-\theta_0\right)^2}{2}\displaystyle\sum_{i=1}^{m}\frac{EI_i r_i\cos\delta_i}{L_i^2} \\ \dfrac{\left(\theta_L-\theta_0\right)^3}{2}\displaystyle\sum_{i=1}^{m}\frac{EI_i r_i\sin\delta_i}{L_i^2} \end{bmatrix} \tag{5}$$

$$\mathbf{J}_{x\psi} = \begin{bmatrix} L_p\cos\delta\dfrac{\left(\theta_L-\theta_0\right)\cos\theta_L-\sin\theta_L+1}{\left(\theta_L-\theta_0\right)^2} & L_p\dfrac{\sin\delta\left(1-\sin\theta_L\right)}{\theta_L-\theta_0} \\ -L_p\sin\delta\dfrac{\left(\theta_L-\theta_0\right)\cos\theta_L-\sin\theta_L+1}{\left(\theta_L-\theta_0\right)^2} & L_p\dfrac{\cos\delta\left(1-\sin\theta_L\right)}{\theta_L-\theta_0} \\ L_p\dfrac{\left(\theta_L-\theta_0\right)\sin\theta_L+\cos\theta_L}{\left(\theta_L-\theta_0\right)^2} & 0 \\ -\sin\delta & \cos\delta\cos\theta_L \\ -\cos\delta & -\sin\delta\cos\theta_L \\ 0 & -1+\sin\theta_L \end{bmatrix} \tag{6}$$

IV. DESIGN DESCRIPTION

The continuum brace from Fig. 1 is used to orient one's limb. Since the upper arm will take up the central space, main design components of this structure include placement and length of the secondary backbones and the actuation unit.

A. Predetermined design parameters

Structure of the continuum brace can be determined by assigning values to length L_p and placement of the secondary backbones (r_i and β_i).

According to Eq. (1), the actuation length of each secondary backbone is only associated with r_i. A different L_p value doesn't affect the bending motion of the continuum brace. Hence, L_p is predetermined to be 120mm. The assumed value is picked to assure the bending radius of each secondary backbone is well above the allowed value according to the material property.

Since a bigger r_i value leads to a bigger q_i for the same amount of bending, a smaller r_i is preferred so that the size of

the actuation unit could be minimized. However, a patient's upper arm should remain inside the continuum brace while performing assisted Activities of Daily Living (ADL). For a specific patient, r_i should be bigger than a minimal value. In order to fit a reasonable group of patients who can perform ADL measured in [41], all the r_i are assumed to be 60mm.

All the predetermined design parameters are summarized in Table II.

TABLE II: PREDETERMINED DESIGN PARAMETERS

$E_p = 60GPa$	$r_i = 60mm$
$E_i = 60GPa$	$L_p = 120mm$

B. Placement of the secondary backbones

There are many possible placements of the secondary backbones in the continuum brace. Different numbers of the secondary backbones could lead to very different designs of actuation units. Hence arrangement of the secondary backbones should be carefully investigated.

In the absence of the primary backbone, at least three secondary backbones are required to orient the upper arm. Actuation of these secondary backbones will bend the continuum brace as well as generate a moment output to drive the patient's upper limb. According to ADL (Activities of Daily Living) measured in [41], a shoulder joint provides a torque as high as 10 Nm to drive the upper limb. Hence the continuum brace should at least have the same capability generating driving torques.

Assume the exoskeleton is assisting a patient with an arm-lifting motion, as shown in Fig. 3. The BDS $\{b\}$ is placed as shown while the configuration of the brace is $\boldsymbol{\psi}=[\pi/6\ \pi]^T$, the exerted external wrench is assumed to be $\mathbf{W}_e=[0\ 0\ 0\ 0\ 10Nm\ 0]^T$.

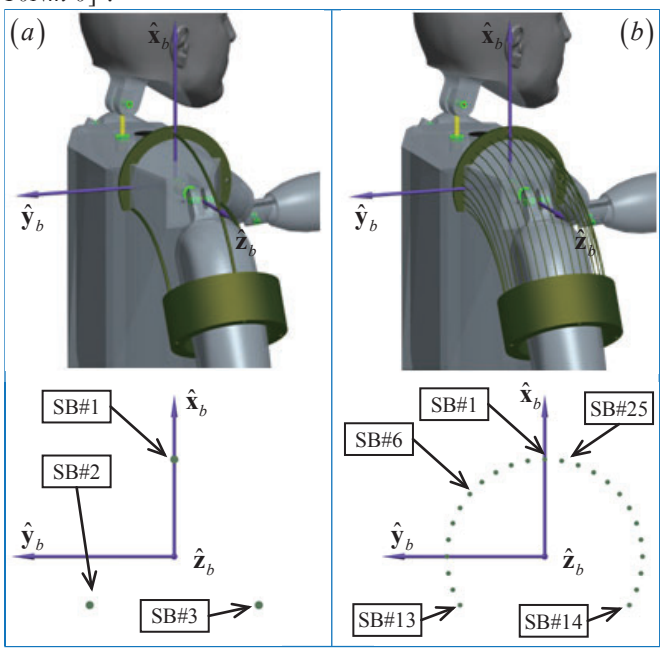

Fig. 3. The continuum brace with different numbers of NiTi backbones: (a) three secondary backbones (b) 25 secondary backbones. Numbering of the Secondary Backbones (shortened as SB) in these two structures is also depicted respectively.

When only three secondary backbones are used, a plot of total stress of secondary backbone 1 can be generated as the backbone's diameter varies from 0.6mm to 3.0mm, as in Fig. 4. The total stress is the sum of two portions, which are the stress due to the push/pull actuation and the stress due to backbone bending. The backbone bending stress linearly increases with an increase in its diameter for a fixed bending curvature.

From various literature [42, 43], stress of the NiTi backbones should be kept under 200MPa ~ 300MPa to safely avoid NiTi's plateau transformation phase. For this reason, the results in Fig. 4 indicate more secondary backbones are preferred to share the load when the exoskeleton is assisting a wearer with daily activities. The more secondary backbones can be used, the thinner each individual secondary backbone is, the more compliant the exoskeleton might feel and the safer the exoskeleton is if one secondary backbone fails.

In the case of using 25 secondary backbones as shown in Fig. 3.(b), the numbering of the secondary backbones is associated with β_i as the following: for SB#1, β_1=0; for SB#2, $\beta_2=\pi/18$; for SB#3, $\beta_3=2\pi/18$; …; for SB#13, $\beta_{13}=12\pi/18$; for SB#14, $\beta_{14}=24\pi/18$; …; for SB#25, $\beta_{25}=35\pi/18$. In this arrangement, 25 secondary backbones are 10° apart spanning $\pm 120°$ in $\{b\}$. The reason of only using 25 secondary backbones is to avoid arranging secondary backbones in oxter so that the wear's upper arm can rest against the trunk.

Another plot can be generated for secondary backbone 1 as in Fig. 5 for the backbone's diameter increases from 0.4mm to 1.2mm for the structure with 25 secondary backbones. Since the total stress is always under 200MPa while picking a thicker backbone could reduce the risk of buckling more, 1.0mm was finally selected as the backbone diameter. In this case, the actuation forces for all the secondary backbones range between -8.91N to 17.82N, while providing an assistive wrench of $\mathbf{W}_e=[0\ 0\ 0\ 0\ 10Nm\ 0]^T$ at the shoulder.

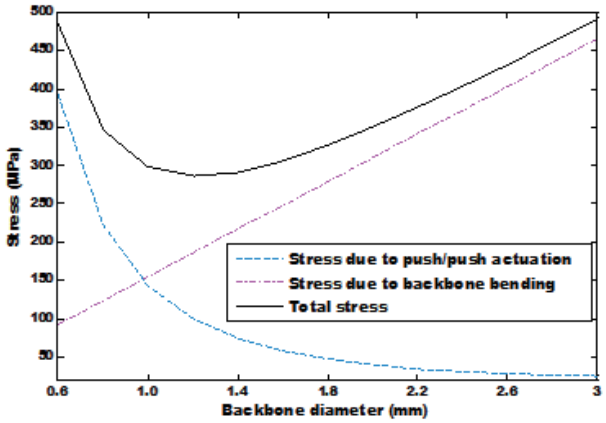

Fig. 4. Calculated stress of secondary backbone 1 in a three-secondary -backbone continuum brace.

C. Design of the Actuation Unit

Using the aforementioned continuum structure with 25 secondary backbones, actuation of the continuum brace involves pulling and pushing 25 thin NiTi backbones simultaneously. Since the structure only possesses two

independent DoFs, using 25 motors to drive these backbones doesn't seem to be an economical solution. A transmission system is needed, taking independent motion inputs from two motors to drive 25 secondary backbones properly.

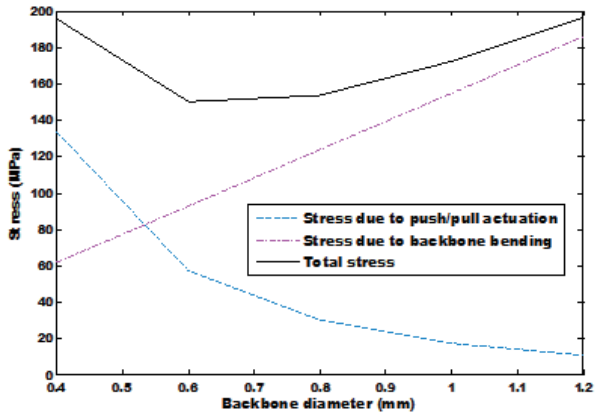

Fig. 5. Calculated stress of secondary backbone 1 in a 25-secondary -backbone continuum brace.

Equation (1) governs the actuation of all the secondary backbones. These actuation values follow a cosine wave with variable amplitudes and phase shifts. A mathematic transformation can be introduced to guide the design of such a transmission mechanism:

$$q_i = \frac{\pi r_i}{2}\cos(\delta + \beta_i)\cos\zeta \tag{7}$$

Where $\zeta = \text{acos}\dfrac{2(\theta_L - \theta_0)}{\pi}$

It can be further transformed as follows:

$$\begin{aligned} q_i &= \frac{\pi r_i}{4}\left(\cos(\delta + \beta_i - \zeta) + \cos(\delta + \beta_i + \zeta)\right) \\ &= \frac{\pi r_i}{4}\left(\cos(\phi_1 + \beta_i) + \cos(\phi_2 + \beta_i)\right) \end{aligned} \tag{8}$$

Where $\phi_1 = \delta - \text{acos}\dfrac{2(\theta_L - \theta_0)}{\pi}$ and $\phi_2 = \delta + \text{acos}\dfrac{2(\theta_L - \theta_0)}{\pi}$

β_i and r_i are constants once the structure is built. If ϕ_1 and ϕ_2 are used as control inputs, each q_i becomes sum of two cosine inputs with a fixed amplitude ($\pi r_i/4$) and a fixed phase offset β_i, according to Eq. (8). Such cosine outputs can be easily generated by a pair of inclined swash plates, as shown in Fig. 6-(b). Then a hydraulic transmission system is designed to realize the addition of the two cosine outputs. As shown in Fig. 6-(a), the paired cosine input pistons are driven up and down by the cylindrical shells from Fig. 6-(b). The liquid pumped from the cylinders equals to the sum of two cosine motions. Then the actuation output piston A will be driven.

According to Eq. (8), two secondary backbones will always have opposite outputs if the difference between their β_i is π. As shown in Fig. 6-(a), the actuation output piston B can be hydraulically connected to the actuation output piston A to always generate opposite outputs.

Mechanisms are also included in the actuation unit to prevent buckling when the secondary backbones are pushed.

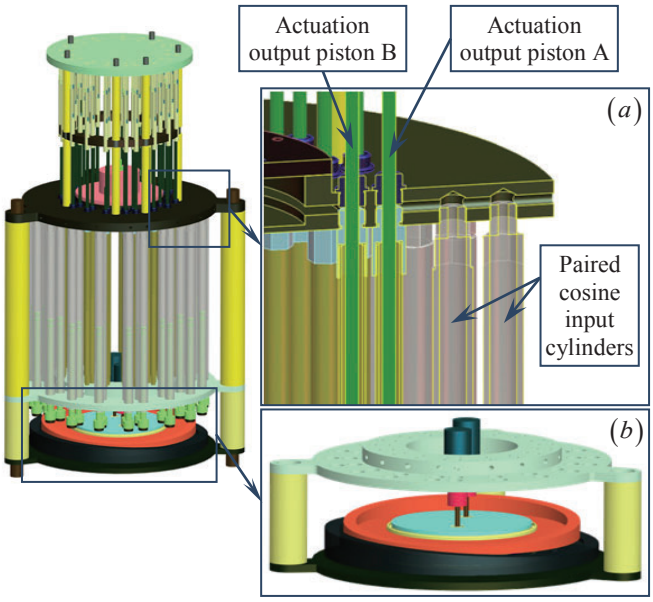

Fig. 6. Actuation unit for the continuum joint brace: (a) a hydraulic transmission system to realize addition of two inputs and (b) cylindrical shells cut at inclination angles to realize cosine outputs.

V. Preliminary Prototype

In order to demonstrate the effectiveness of the proposed exoskeleton design, a mockup model of a trunk, an upper arm and a shoulder joint was constructed as shown in Fig. 7.(a). The shoulder joint is formed by two revolute joints connected in serial. Although a spherical joint better mimics a human shoulder joint, the current form of the shoulder joint has a bigger motion range for better demonstration.

As shown in Fig. 7-(b) to Fig. 7-(d), a mockup exoskeleton was put on the upper arm and the shoulder. An inflatable bandage was inserted between the upper arm and the arm sleeve so that motion of the upper arm sleeve could be transmitted to the upper arm.

In the absence of an actuation unit, all the secondary backbones were manually pushed or pulled. At a specific configuration of the continuum brace, the actuation length q_i is maintained by clamping the corresponding secondary backbones.

With the assistance of the mockup exoskeleton, the upper arm can be lifted, pointing at an arbitrary direction. However, the current form of the shoulder joint generates some kinematic discrepancy between the upper arm and the upper arm sleeve of the exoskeleton (the difference is a rotation along the axis of the upper arm). Small pulleys are assembled into the upper arm sleeve. When this kinematic discrepancy occurs, the upper arm sleeve can rotate freely with respect to the inflatable bandage.

VI. Conclusion and Future Work

This paper presented a design alternative for rehabilitation exoskeletons using flexible continuum mechanisms, in order to address user needs for ergonomics, comfort, low inertia, device compactness.

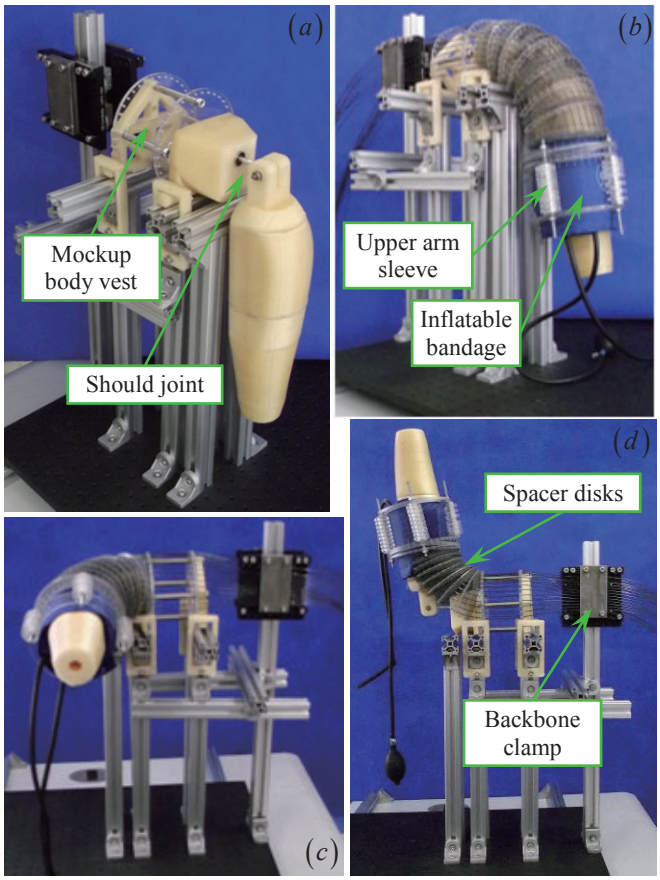

Fig. 7. A mockup model of a shoulder and an upper arm with and without the exoskeleton worn

This design concept was first applied to an upper extremity exoskeleton for a shoulder joint. Actuating the continuum mechanism will orient a wearer's upper arm accordingly. Design considerations were carefully discussed based on a more general kinematics and statics model extended from previously published results. A specific structure of the continuum mechanism is selected weighing these design considerations. Actuation and transmission schemes for the selected structure were also presented.

After the feasibility of the proposed idea is demonstrated using a preliminary prototype, future work includes fabricating and assembling all the mechanical components and building a motorized control system. It is foreseeable that there will be discrepancy between the theoretic kinematics model and the actual motion of the upper arm. Compensation algorithms would be considered by specific design of the swash plates that allow changes in the inclination angle.

REFERENCES

[1] B. R. Brewer, S. K. McDowell, and L. C. Worthen-Chaudhari, "Poststroke Upper Extremity Rehabilitation: A Review of Robotic Systems and Clinical Results," *Topics in Stroke Rehabilitation,* vol. 14, pp. 22-44, Nov 2007.

[2] A. M. Dollar and H. Herr, "Lower Extremity Exoskeletons and Active Orthoses: Challenges and State-of-the-Art," *IEEE Transactions on Robotics,* vol. 24, pp. 144-158, Feb 2008.

[3] M. Vukobratovic, D. Hristic, and Z. Stojiljkovic, "Development of Active Anthropomorphic Exoskeletons," *Medical and Biological Engineering and Computing,* vol. 12, pp. 66-80, Jan 1974.

[4] H. Kawamoto, S. Lee, S. Kanbe, and Y. Sankai, "Power Assist Method for HAL-3 using EMG-based Feedback Controller," in *IEEE International Conference on Systems, Man and Cybernetics (IEEE SMC)*, Washington, D.C., USA, 2003, pp. 1648-1653.

[5] K. Yamamoto, M. Ishii, H. Noborisaka, and K. Hyodo, "Stand Alone Wearable Power Assisting Suit: Sensing and Control Systems," in *IEEE International Workshop on Robot and Human Interactive Communication*, Kurashiki, Okayama, Japan, 2004.

[6] E. Guizzo and H. Goldstein, "The Rise of the Body Bots," *IEEE Spectrum,* vol. 42, pp. 42-48, Oct 2005.

[7] A. B. Zoss, H. Kazerooni, and A. Chu, "Biomechanical Design of the Berkeley Extremity Exoskeleton (BLEEX)," *IEEE/ASME Transaction on Mechatronics,* vol. 11, pp. 128-138, April 2006.

[8] C. J. Walsh, D. Paluska, K. Pasch, W. Grand, A. Valiente, and H. Herr, "Development of a Lightweight, Underactuated Exoskeleton for Load-Carrying Augmentation," in *IEEE International Conference on Robotics and Automation (ICRA)*, Orlando, Florida, USA, 2006.

[9] W. K. Durfee and A. Rivard, "Priliminary Design and Simulation of a Pneumatic, Stored-Energy, Hybrid Orthosis for Gait Restoration," in *ASME International Mechanical Engineering Congress*, Anaheim, California USA, 2004, pp. 1-7.

[10] S. K. Banala, S. K. Agrawal, A. Fattah, V. Krishnamoorthy, W.-L. Hsu, J. Scholz, and K. Rudolph, "Gravity-Balancing Leg Orthosis and Its Performance Evaluation," *IEEE Transactions on Robotics,* vol. 22, pp. 1228-1239, 2006.

[11] J. F. Veneman, R. Ekkelenkamp, R. Kruidhof, F. C. T. van der Helm, and H. van der Kooij, "A Series Elastic- and Bowden-Cable-Based Actuation System for Use as Torque Actuator in Exoskeleton-Type Robots," *International Journal of Robotics Research,* vol. 25, pp. 261-281, March 2006.

[12] J. A. Saglia, N. G. Tsagarakis, J. S. Dai, and D. G. Caldwell, "A High Performance 2-dof Over-Actuated Parallel Mechanism for Ankle Rehabilitation," in *IEEE International Conference on Robotics and Automation (ICRA)*, Kobe, Japan, 2009, pp. 2180-2186.

[13] N. G. Tsagarakis and D. G. Caldwell, "Development and Control of a 'Soft-Actuated' Exoskeleton for Use in Physiotherapy and Training," *Autonomous Robots,* vol. 15, pp. 21-33, 2003.

[14] J. C. Perry, J. Rosen, and S. Burns, "Upper-Limb Powered Exoskeleton Design," *IEEE/ASME Transaction on Mechatronics,* vol. 12, pp. 408-417, Aug 2007.

[15] R. C. V. Loureiro and W. S. Harwin, "Reach & Grasp Therapy: Design and Control of a 9-DOF Robotic Neuro-rehabilitation System," in *IEEE International Conference on Rehabilitation Robotics*, Noordwijk, The Netherlands, 2007, pp. 757-763.

[16] A. Gupta, M. K. O'Malley, V. Patoglu, and C. Burgar, "Design, Control and Performance of RiceWrist: A Force Feedback Wrist Exoskeleton for Rehabilitation and Training," *International Journal of Robotics Research,* vol. 27, pp. 233-251, Feb 2008.

[17] A. H. A. Stienen, E. E. G. Hekman, G. B. Prange, M. J. A. Jannink, A. M. M. Aalsma, F. C. T. v. d. Helm, and H. v. d. Kooij, "Dampace: Design of an Exoskeleton for Force-Coordination Training in Upper-Extremity Rehabilitation," *Journal of Medical Devices,* vol. 3, pp. 1-10, Sept 2009.

[18] M. Fontana, A. Dettori, F. Salsedo, and M. Bergamasco, "Mechanical Design of a Novel Hand Exoskeleton for Accurate Force Displaying," in *IEEE International Conference on Robotics and Automation (ICRA)*, Kobe, Japan, 2009, pp. 1704-1709.

[19] J. Klein, S. Spencer, J. Allington, J. E. Bobrow, and D. J. Reinkensmeyer, "Optimization of a Parallel Shoulder Mechanism to Achieve a High-Force, Low-Mass, Robotic-Arm Exoskeleton," *IEEE Transactions on Robotics,* vol. 26, pp. 710-715, Aug 2010.

[20] E. T. Wolbrecht, D. J. Reinkensmeyer, and J. E. Bobrow, "Pneumatic Control of Robots for Rehabilitation," *International Journal of Robotics Research,* vol. 29, pp. 23-38, Jan 2010.

[21] J. Oblak, I. Cikajlo, and Z. Matjacic, "Universal Haptic Drive: A Robot for Arm and Wrist Rehabilitation," *IEEE Transactions on Neural Systems and Rehabilitation Engineering,* vol. 18, pp. 293-302, June 2010.

[22] G. Aguirre-Ollinger, J. E. Colgate, M. A. Peshkin, and A. Goswami, "Design of an Active One-Degree-of-Freedom Lower-Limb Exoskeleton with Inertia Compensation," *International Journal of Robotics Research,* vol. onlinefirst, Dec 2010.

[23] C. Fleischer and G. Hommel, "A Human–Exoskeleton Interface Utilizing Electromyography," *IEEE Transactions on Robotics,* vol. 24, pp. 872-882, Aug 2008.
[24] V. Sharma, D. B. McCreery, M. Han, and V. Pikov, "Bidirectional Telemetry Controller for Neuroprosthetic Devices," *IEEE Transactions on Neural Systems and Rehabilitation Engineering,* vol. 18, pp. 67-74, Feb 2010.
[25] A. Schiele and F. C. T. van der Helm, "Kinematic Design to Improve Ergonomics in Human Machine Interaction," *IEEE Transactions on Neural Systems and Rehabilitation Engineering,* vol. 14, pp. 456-469, Dec 2006.
[26] N. Jarrassé and G. Morel, "A Formal Method for Avoiding Hyperstaticity When Connecting an Exoskeleton to a Human Member," in *IEEE International Conference on Robotics and Automation (ICRA)*, Anchorage, AK, USA, 2010, pp. 1188-1195.
[27] A. H. A. Stienen, E. E. G. Hekman, H. t. Braak, A. M. M. Aalsma, F. C. T. v. d. Helm, and H. v. d. Kooij, "Design of a Rotational Hydroelastic Actuator for a Powered Exoskeleton for Upper Limb Rehabilitation," *IEEE Transactions on Biomedical Engineering,* vol. 57, pp. 728-735, March 2010.
[28] K. Kong, H. Moon, B. Hwang, D. Jeon, and M. Tomizuka, "Robotic Rehabilitation Treatments: Realization of Aquatic Therapy Effects in Exoskeleton Systems," in *IEEE International Conference on Robotics and Automation (ICRA)*, Kobe, Japan, 2009, pp. 1923-1928.
[29] A. Duschau-Wicke, J. v. Zitzewitz, A. Caprez, L. Lünenburger, and Robert Riener, "Path Control: A Method for Patient-Cooperative Robot-Aided Gait Rehabilitation," *IEEE Transactions on Neural Systems and Rehabilitation Engineering,* vol. 18, pp. 38-48, Feb 2010.
[30] A. J. van den Bogert, "Exotendons for assistance of human locomotion," *Biomedical Engineering Online,* vol. 2, Oct 2003.
[31] H. Kobayashi and K. Hiramatsu, "Development of Muscle Suit for Upper Limb," in *IEEE International Conference on Robotics and Automation (ICRA)*, New Orleans, LA, USA, 2004, pp. 2480-2485.
[32] S. K. Agrawal, V. N. Dubey, J. J. Gangloff, E. Brackbill, Y. Mao, and V. Sangwan, "Design and Optimization of a Cable Driven Upper Arm Exoskeleton," *Journal of Medical Devices,* vol. 3, pp. 1-8, Sept 2009.
[33] E. A. Brackbill, Y. Mao, S. K. Agrawal, M. Annapragada, and V. N. Dubey, "Dynamics and Control of a 4-dof Wearable Cable-driven Upper Arm Exoskeleton," in *IEEE International Conference on Robotics and Automation (ICRA)*, Kobe, Japan, 2009, pp. 2300-2305.
[34] K. Xu and N. Simaan, "An Investigation of the Intrinsic Force Sensing Capabilities of Continuum Robots," *IEEE Transactions on Robotics,* vol. 24, pp. 576-587, June 2008.
[35] N. Simaan, K. Xu, A. Kapoor, W. Wei, P. Kazanzides, P. Flint, and R. H. Taylor, "Design and Integration of a Telerobotic System for Minimally Invasive Surgery of the Throat " *International Journal of Robotics Research,* vol. 28, pp. 1134-1153, 2009.
[36] K. Xu and N. Simaan, "Analytic Formulation for the Kinematics, Statics and Shape Restoration of Multibackbone Continuum Robots via Elliptic Integrals," *Journal of Mechanisms and Robotics,* vol. 2, Feb 2010.
[37] I. A. Gravagne and I. D. Walker, "Manipulability, Force and Compliance Analysis for Planar Continuum Manipulators," *IEEE Transactions on Robotics and Automation,* vol. 18, pp. 263-273, Jun 2002.
[38] B. A. Jones and I. D. Walker, "Kinematics for Multisection Continuum Robots," *IEEE Transactions on Robotics and Automation,* vol. 22, pp. 43-55, Feb 2006.
[39] K. Xu and N. Simaan, "Actuation Compensation for Flexible Surgical Snake-like Robots with Redundant Remote Actuation," in *IEEE International Conference on Robotics and Automation (ICRA)*, Orlando, Florida, USA, 2006, pp. 4148- 4154.
[40] R. J. Webster and B. A. Jones, "Design and Kinematic Modeling of Constant Curvature Continuum Robots: A Review," *The International Journal of Robotics Research,* June 2010.
[41] J. Rosen, J. C. Perry, N. Manning, S. Burns, and B. Hannaford, "The Human Arm Kinematics and Dynamics during Daily Activities - toward a 7 DOF Upper Limb Powered Exoskeleton," in *IEEE International Conference on Advanced Robotics (ICAR)*, Seattle, WA, 2005, pp. 532-539.
[42] R. Matsui, H. Tobushi, Y. Furuichi, and H. Horikawa, "Tensile Deformation and Rotating-Bending Fatigue Properties of a Highelastic Thin Wire, a Superelastic Thin Wire, and a Superelastic Thin Tube of NiTi Alloys," *Journal of Engineering Materials and Technology,* vol. 126, pp. 384-391, Oct 2004.
[43] J. A. Shaw and S. Kyriakides, "Thermomechanical Aspects of NiTi," *Journal of the Mechanics and Physics of Solids,* vol. 43, pp. 1243-1281, Aug 1995.